Journal of Computational and Graphical Statistics

ISSN: 1061-8600 (Print) 1537-2715 (Online) Journal homepage: www.tandfonline.com/journals/ucgs20

The Torgegram for Fluvial Variography: Characterizing Spatial Dependence on Stream Networks

Dale L. Zimmerman & Jay M. Ver Hoef

To cite this article: Dale L. Zimmerman & Jay M. Ver Hoef (2017) The Torgegram for Fluvial Variography: Characterizing Spatial Dependence on Stream Networks, Journal of Computational and Graphical Statistics, 26:2, 253-264, DOI: 10.1080/10618600.2016.1247006

To link to this article: https://doi.org/10.1080/10618600.2016.1247006

JOURNAL OF COMPUTATIONAL AND GRAPHICAL STATISTICS
2017, VOL. 26, NO. 2, 253–264
http://dx.doi.org/10.1080/10618600.2016.1247006

Taylor & Francis
Taylor & Francis Group

The Torgegram for Fluvial Variography: Characterizing Spatial Dependence on Stream Networks

Dale L. Zimmerman [a] and Jay M. Ver Hoef[b]

[a]Department of Statistics and Actuarial Science, University of Iowa, Iowa City, Iowa; [b]NOAA-NMFS Alaska Fisheries Science Center, Marine Mammal Laboratory, Seattle, Washington

ABSTRACT

We introduce a graphical diagnostic called the Torgegram for characterizing spatial dependence among observations of a variable on a stream network. The Torgegram consists of four component empirical semivariograms, each one corresponding to a particular combination of flow-connectedness within the network and model type (tail-up/tail-down). We show how an overall strategy for fluvial variography can be based on a careful examination of the Torgegram. An analysis of water temperature data from a stream network within the Columbia River basin of the northwest United States illustrates the diagnostic value of the Torgegram as well as its limitations. Additional uses and extensions of the Torgegram are discussed.

ARTICLE HISTORY
Received February 2016
Revised August 2016

KEYWORDS
Geostatistics; Semivariogram; Spatial covariance; Tail-down model; Tail-up model

1. Introduction

Streams and rivers are an important environmental resource. Consequently, major efforts are ongoing to characterize and monitor streams and rivers throughout the world (see, e.g., Bunn et al. 2010; Chandler et al. 2016; Wang et al. 2011; McKay et al. 2012). As with most environmental monitoring studies, monitoring a stream variable requires that a sample be taken from a possibly infinite population of values on a stream network. The sample could consist, for example, of water quality measurements at discrete point sites on the network, or counts of fish from short stream sections. The inferential goals for stream variables may vary, but often include predicting values of the variable(s) at unsampled locations, predicting an average value or total for a stream segment or the entire stream network, estimating the effects of covariate (fixed) effects on response variables from streams, and estimating temporal trends.

Spatial statistical methods for achieving the inferential goals just mentioned have been available for a long time for data from Euclidean (rather than stream network) domains, and are known collectively as geostatistics. In the geostatistical paradigm, the observed data are regarded as a sample taken from one realization of a stochastic process indexed by points in Euclidean space, that is, as $Y(\cdot) \equiv \{Y(\mathbf{s}) : \mathbf{s} \in D\}$ where D is a region in two-dimensional (usually) Euclidean space, and $\mathbf{s}$ is a point location in that region. It is often assumed, unless there is evidence to the contrary, that the stochastic process is intrinsically stationary and isotropic, that is, that its mean is constant across space and its second-order dependence, as characterized by the semivariogram $\gamma(\mathbf{s}, \mathbf{t}) \equiv \frac{1}{2}E[Y(\mathbf{s}) - Y(\mathbf{t})]^2$, may be expressed as a function of the Euclidean distance, $h = \|\mathbf{s} - \mathbf{t}\|$, between locations. Before the aforementioned inferential goals can be achieved, the semivariogram must be estimated, characterized, and modeled—an exercise known as *variography*.

The main tool of variography is the empirical semivariogram, defined as

$$\hat{\gamma}(h_k) = \frac{1}{2N(\mathcal{H}_k)} \sum_{\|\mathbf{s}_i - \mathbf{s}_j\| \in \mathcal{H}_k} (Y(\mathbf{s}_i) - Y(\mathbf{s}_j))^2, \quad k = 1, \ldots, K, \tag{1}$$

where $Y(\mathbf{s}_1), \ldots, Y(\mathbf{s}_n)$ are the observed data, h_k is a representative distance (often the average or midrange) for a distance bin $\mathcal{H}_k$, and $N(\mathcal{H}_k)$ is the number of distinct site-pairs in $\mathcal{H}_k$. From a plot of $\hat{\gamma}(h_k)$ versus h_k, the analyst can often discern important features of the semivariogram, including the following: a *sill* (the limit of $\gamma(h)$ as $h \to \infty$, if this limit exists), which is equivalent to the variance of $Y(\cdot)$; a *range* (the distance at which the sill is reached, or equivalently the distance beyond which the correlation is essentially zero, if such a distance exists); a *nugget* (the limit of $\gamma(h)$ as $h \to 0$); and various shape attributes (e.g., sigmoidicity, concavity, monotonicity, or periodicity).

Furthermore, the empirical semivariogram and/or simple extensions of it can be used to check the underlying assumptions of second-order stationarity and isotropy. For example, an empirical semivariogram that appears to increase without bound is evidence that $Y(\cdot)$ is not second-order stationary, possibly because its mean is not constant—a phenomenon known as *trend contamination*. Another possible manifestation of nonstationarity is a sill and/or range that varies over space. Region-specific empirical semivariograms, computed from observations taken in disjoint subregions of the spatial domain, may be compared to look for this type of nonstationarity. Similarly, direction-specific empirical semivariograms may be compared to assess the isotropy assumption. Formal tests for second-order stationarity and isotropy can be based on these extended semivariograms; see Jun and Genton (2012) and Guan, Sherman, and Calvin (2004).

CONTACT Dale L. Zimmerman dale-zimmerman@uiowa.edu Department of Statistics and Actuarial Science, University of Iowa, Iowa City, IA 52242, USA.
Color versions of one or more of the figures in the article can be found online at www.tandfonline.com/r/JCGS.

Because geostatistical methods have been so successful for analyzing data in Euclidean spatial domains, there have recently been several attempts to apply them to data from stream networks also, with *stream distance* (distance along the stream network) replacing Euclidean distance in the semivariogram; for examples of such applications see Legleiter et al. (2003), Torgersen, Gresswell, and Bateman (2004), Yuan (2004), Ganio, Torgersen, and Gresswell (2005), Peterson and Urquhart (2006), and Money, Carter, and Serre (2009). However, semivariogram models that correspond to valid (positive definite) covariance functions in two- and three-dimensional Euclidean space are not necessarily valid when stream distance is substituted for Euclidean distance, an issue that continues to be ignored by some authors, for example, Okabe and Sugihara (2012, chap. 10). Furthermore, because streams have flow, which is characterized by direction and volume, for some stream variables it may not be appropriate to model spatial correlation as a function of stream distance alone. Within the past decade, positive definite covariance models on stream networks that incorporate flow direction and volume have been introduced (Ver Hoef, Peterson, and Theobald 2006; Cressie et al. 2006; Ver Hoef and Peterson 2010). The models are based on unilateral moving average constructions and can be categorized as either "tail-up" or "tail-down." Under a tail-up model, variables at sites that are not connected by flow (e.g., sites on two branches upstream from their junction) are uncorrelated. In contrast, tail-down models allow for correlation between variables at all sites on the same network, regardless of whether they are flow-connected.

Although valid geostatistical models for stream variables are now available, relatively little attention has been given to the development of graphical tools analogous to the Euclidean distance-based empirical semivariogram for variography on stream networks, or *fluvial* variography. In this article, we develop such a tool, which we call the Torgegram. The Torgegram is an assemblage of four empirical semivariograms, each one relevant to a particular combination of flow-connectedness and model type (tail-up/tail-down).

The remainder of the article is organized as follows. In Section 2, we review some elementary stream network topology and covariance models on stream networks, in particular those based on the unilateral moving average constructions of Ver Hoef and Peterson (2010). Section 3 presents the Torgegram in detail and describes a strategy for fluvial variography based upon it. An example for a stream temperature dataset from within the Columbia River basin is presented in Section 4, and Section 5 is a discussion.

2. Spatial Models on Stream Networks

2.1 Stream Network Topology and Notation

Ver Hoef, Peterson, and Theobald (2006) set forth a number of topological concepts for stream networks. Here, we briefly review those concepts that are necessary for our purposes.

A stream network may be conceptualized as a directed acyclic graph with nodes defined by stream junctions (locations where two or more streams join), edges defined by stream segments between junctions, and the directions of the edges defined by the direction that the water flows. We assume that the network is strictly dendritic, that is, it includes no braided streams. We also assume that the network has no river delta, in which case it has a single furthest downstream point, the "outlet," whose spatial coordinate is set to 0. Any location in the network can be connected to the outlet by a continuous curve along the network, and the length of that curve is called the "upstream distance" of that location. To uniquely define individual locations and keep track of their upstream distances, each location is denoted by s_i, where i indicates that the location is on the ith stream segment, and s is its upstream distance. Thus, two locations may be distinct but nevertheless have the same upstream distance. The "stream distance" between locations s_i and t_j is the shortest distance between them through the network, and is denoted by $d(s_i, t_j)$.

For each s_i, let U_i denote the set of stream segments that lie upstream of s_i, including the ith segment. Locations s_i and t_j are said to be "flow-unconnected" if $U_i \cap U_j = \emptyset$, and are "flow-connected" otherwise. If locations s_i and t_j are flow-connected, then $d(s_i, t_j) = |s - t|$. On the other hand, if s_i and t_j are flow-unconnected, then $d(s_i, t_j) = (s - q_{ij}) + (t - q_{ij})$, where q_{ij} is the upstream distance of the "common junction" of segments i and j, that is, the junction where flows from segments i and j first combine. When s_i and t_j are flow-unconnected, we refer to $d(s_i, t_j)$ as the "total stream distance" between them.

2.2 Covariance Models

The classical geostatistical model, adapted for use with a stream variable $Y(\cdot)$, is given by

$$Y(s_i) = \mu + \epsilon(s_i), \tag{2}$$

where μ, the mean of $Y(\cdot)$, is assumed to be constant (though this assumption can be relaxed with little difficulty) and $\epsilon(\cdot)$ is a zero-mean residual stochastic process on the stream network whose distribution is a function of an unknown finite parameter vector $\boldsymbol{\theta}$. For spatial analysis in general, and spatial prediction via best linear unbiased prediction (kriging) in particular, the second-order dependence (i.e., covariance) structure of $Y(\cdot)$, as characterized by $\boldsymbol{\theta}$ or functions thereof, plays a huge role. A classical approach to the development of covariance functions on the real line is to create model residuals as integrations of a moving-average function over a white-noise random process, that is,

$$\epsilon(s|\boldsymbol{\theta}) = \int_{-\infty}^{\infty} g(x - s|\boldsymbol{\theta}) dW(x),$$

where x and s are locations and $g(x|\boldsymbol{\theta})$ is a square-integrable moving average function defined on the real line (Yaglom 1987). The covariance between $\epsilon(s)$ and $\epsilon(s + h)$ so defined is given by

$$C(h|\boldsymbol{\theta}) = \int_{-\infty}^{\infty} g(x|\boldsymbol{\theta}) g(x - h|\boldsymbol{\theta}) dx.$$

Appropriate choices of the moving average function yield many of the covariance functions commonly used in Euclidean geostatistics (spherical, exponential, etc.).

Cressie et al. (2006), Ver Hoef, Peterson, and Theobald (2006), and Ver Hoef and Peterson (2010) obtained covariance models for stream network variables by adapting this classical

approach to the unique topology of stream networks. They considered in particular only *unilateral* models, that is, those models that arise by taking the moving-average function to be positive in only one direction (either upstream or downstream) and zero elsewhere. Considering those moving average functions that are positive only upstream, and weighting at each junction to achieve variance stationarity, we obtain the class of "tail-up" covariance functions

$$C_{tu}(s_i, t_j|\{\pi_{ij}\}, \boldsymbol{\theta}) = \begin{cases} \pi_{ij} C_{uw}(s - t|\boldsymbol{\theta}) & \text{if } s_i \geq t_j \text{ are flow-connected,} \\ 0 & \text{if } s_i \text{ and } t_j \text{ are flow-unconnected,} \end{cases} \quad (3)$$

where the π_{ij}'s are spatial weights and $C_{uw}(\cdot)$, which we call the *unweighted* flow-connected portion of a tail-up covariance function, is a valid covariance function on the real line. The spatial weights, more precisely, are given by $\pi_{ij} = \prod_{k \in B_{ij}} \sqrt{\omega_k}$ where B_{ij} is the set of segments that lie between the ith and jth, including the jth but excluding the ith (the jth being downstream of the ith), and ω_k is any attribute of the kth segment (e.g., watershed area, flow volume, stream order, stream slope) expressed as a proportion. Often, it may be desirable to take ω_k to be the proportion of flow volume contributed by the kth segment to the junction at its downstream terminus, but flow volume is rarely available so watershed area, which is easily obtained via a GIS, may be used as a surrogate. The lack of correlation between observations on flow-unconnected segments and the explicit account taken of flow volume (or a surrogate for it) make tail-up models seem especially appropriate for variables such as concentrations of point-source pollutants, which generally move passively downstream.

On the other hand, moving average functions that are positive only in the downstream direction yield the class of "tail-down" covariance functions

$$C_{td}(s_i, t_j|\boldsymbol{\theta}) = \begin{cases} C_{fc}(s - t|\boldsymbol{\theta}) & \text{if } s_i \geq t_j \text{ are flow-connected,} \\ C_{fu}(s - q_{ij}, t - q_{ij}|\boldsymbol{\theta}) & \text{if } s_i \text{ and } t_j \text{ are flow-unconnected,} \end{cases} \quad (4)$$

where $C_{fc}(\cdot)$ and $C_{fu}(\cdot)$ are valid covariance functions of one and two variables, respectively (and are related to each other through their functional dependence on the same moving average function). Thus, the flow-connected portion of a tail-down covariance function is a function of the stream distance between locations, but the flow-unconnected portion is a function of the two stream distances to the common junction. No weighting by flow (or anything else) is associated with tail-down models. Because they allow for positive correlation among both flow-connected and flow-unconnected sites on the same network, tail-down models would appear to be more well-suited than tail-up models for counts of fish and some insects, which can move both upstream and downstream.

Some examples of tail-up and tail-down models are listed in Table 1. The tail-down exponential model is noteworthy for being the only model for which the dependence on the two distances to common junction in the flow-unconnected portion is additive. Two-tailed models (for which the moving average function is bilateral, but not necessarily symmetric about 0) can also be defined, but severe computational issues associated with them have led researchers to consider mixed linear models with tail-up and tail-down components as a more convenient alternative (Ver Hoef and Peterson 2010). A general mixed model of this type is given by

$$\epsilon(s_i) = \epsilon_{tu}(s_i) + \epsilon_{td}(s_i) + \nu(s_i), \quad (5)$$

where $\epsilon_{tu}(\cdot)$, $\epsilon_{td}(\cdot)$, and $\nu(\cdot)$ are uncorrelated with each other and have pure tail-up, pure tail-down, and pure nugget covariance functions, respectively. Observations with errors that follow this model have a covariance matrix given by

$$\begin{aligned} \boldsymbol{\Sigma}(\boldsymbol{\theta}) &= \boldsymbol{\Sigma}((\sigma^2_{tu}, \sigma^2_{td}, \sigma^2_{nu}, \boldsymbol{\rho}'_{tu}, \boldsymbol{\rho}'_{td})') \\ &= \sigma^2_{tu}\mathbf{R}_{tu}(\boldsymbol{\rho}_{tu}) + \sigma^2_{td}\mathbf{R}_{td}(\boldsymbol{\rho}_{td}) + \sigma^2_{nu}\mathbf{I}, \end{aligned} \quad (6)$$

where $\mathbf{R}_{tu}(\boldsymbol{\rho}_{tu})$ is a matrix of autocorrelation values from the tail-up component; $\mathbf{R}_{td}(\boldsymbol{\rho}_{td})$ is a matrix of autocorrelation values from the tail-down component; $\mathbf{I}$ is an identity matrix; σ^2_{tu}, σ^2_{td}, and σ^2_{nu} (the nugget effect) are variance components; and $\boldsymbol{\rho}_{tu}$ and $\boldsymbol{\rho}_{td}$ are vectors of correlation parameters.

The preceding has focused on covariance models. For various reasons, practitioners of Euclidean geostatistics have preferred to characterize second-order dependence via the semivariogram instead. For processes having stationary variances, however, there is a one-to-one correspondence between the covariance function and semivariogram. Likewise, for every mixed-model stream-network covariance function, there is a corresponding semivariogram, given by the relationship

$$\gamma(s_i, t_j) = \sigma^2_{tu} + \sigma^2_{td} + \sigma^2_{nu} - C_{tu}(s_i, t_j) - C_{td}(s_i, t_j).$$

In what follows, we base our consideration of fluvial variography on such semivariograms rather than the corresponding covariance functions.

3. The Torgegram

From Section 2.2, it is clear that for tail-up and tail-down covariance models (and mixtures thereof) on stream networks, the correlation among responses may depend not only on total stream distance but also on flow connectedness, flow volume, and/or distances to a common junction. Thus, in contrast to Euclidean geostatistics, one empirical semivariogram is not adequate for characterizing spatial dependence on a stream network. Instead, no less than four distinct empirical semivariograms, each a modification of the Euclidean empirical semivariogram, may be necessary. We call this quadripartite collection of empirical semivariograms the *Torgegram* in honor of Christian Torgersen, a stream ecologist who was among the first to study spatial dependence on streams.

3.1 Four Components

3.1.1 The Flow-Unconnected Stream-Distance (FUSD) Semivariogram

As its name suggests, this empirical semivariogram is computed from only those site-pairs that are flow-unconnected and, for such pairs, is a function of total stream distance only. It is defined

Table 1. Examples of tail-up and tail-down covariance models. For the tail-up models, only the unweighted flow-connected portion is displayed; the complete model is given by substitution in (3). For all models, it is assumed that $s \geq t$ without loss of generality, and we write $h = s - t$.

Name	Functional form
Tail-up linear with sill	$C_{uu}(h\|\theta_1, \theta_2) = \theta_1 \left(1 - \frac{h}{\theta_2}\right) I\left(\frac{h}{\theta_2} \leq 1\right)$
Tail-up spherical	$C_{uu}(h\|\theta_1, \theta_2) = \theta_1 \left(1 - \frac{3h}{2\theta_2} + \frac{h^3}{\theta_2^3}\right) I\left(\frac{h}{2\theta_2} \leq 1\right)$
Tail-up exponential	$C_{uu}(h\|\theta_1, \theta_2) = \theta_1 \exp(-h/\theta_2)$
Tail-up Mariah	$C_{uu}(h\|\theta_1, \theta_2) = \begin{cases} \theta_1 & \text{if } h = 0 \\ \theta_1 \left(\frac{\log(1 + h/\theta_2)}{h/\theta_2}\right) & \text{if } h > 0 \end{cases}$
Tail-down linear with sill	$C_{td}(s_i, t_j\|\theta_1, \theta_2) = \begin{cases} \theta_1 \left(1 - \frac{h}{\theta_2}\right) I\left(\frac{h}{\theta_2} \leq 1\right) & \text{if flow-connected} \\ \theta_1 \left(1 - \frac{s - q_{ij}}{\theta_2}\right) I\left(\frac{s - q_{ij}}{\theta_2} \leq 1\right) & \text{if flow-unconnected} \end{cases}$
Tail-down spherical	$C_{td}(s_i, t_j\|\theta_1, \theta_2) = \begin{cases} \theta_1 \left(1 - \frac{3h}{2\theta_2} + \frac{h^3}{2\theta_2^3}\right) I\left(\frac{h}{\theta_2} \leq 1\right) & \text{if flow-connected} \\ \theta_1 \left(1 - \frac{3(t - q_{ij})}{2\theta_2} + \frac{s - q_{ij}}{2\theta_2}\right) \left(1 - \frac{s - q_{ij}}{\theta_2}\right)^2 I\left(\frac{s - q_{ij}}{\theta_2} \leq 1\right) & \text{if flow-unconnected} \end{cases}$
Tail-down exponential	$C_{td}(s_i, t_j\|\theta_1, \theta_2) = \theta_1 \exp(-h/\theta_2)$
Tail-down Mariah	$C_{td}(s_i, t_j\|\theta_1, \theta_2) = \begin{cases} \theta_1 & \text{if flow-connected and } h = 0 \\ \theta_1 \left(\frac{\log(1 + h/\theta_2)}{h/\theta_2}\right) & \text{if flow-connected and } h > 0 \\ \theta_1 \left(\frac{1}{1 + (t - q_{ij})/\theta_2}\right) & \text{if flow-unconnected and } s = t \\ \theta_1 \left(\frac{\log(1 + (s - q_{ij})/\theta_2) - \log(1 + (t - q_{ij})/\theta_2)}{(s - t)/\theta_2}\right) & \text{if flow-unconnected and } s \neq t \end{cases}$

formally as

$$\hat{\gamma}_{\text{FUSD}}(h_k) = \frac{1}{2N(\mathcal{U}_k)} \sum_{(s_i, t_j) \in \mathcal{U}_k} (Y(s_i) - Y(t_j))^2, \quad k = 1, \ldots, K_{\mathcal{U}}, \tag{7}$$

where $\mathcal{U}_k = \{(s_i, t_j) : d(s_i, t_j) \in \mathcal{H}_k,\ U_i \cap U_j = \emptyset\}$, $\{\mathcal{H}_k : k = 1, \ldots, K\}$ is a partition of the total stream distances into bins, h_k is a representative distance within $\mathcal{U}_k$, $N(\mathcal{U}_k)$ is the number of distinct site-pairs in $\mathcal{U}_k$, and $K_{\mathcal{U}}$ is the number of stream-distance bins for those site-pairs. If $Y(\cdot)$ is pure tail-up, then $\hat{\gamma}_{\text{FUSD}}(\cdot)$ is unbiased (apart from a "blurring" effect due to binning similar but unequal total stream distances) for the flow-unconnected portion of its semivariogram, which in this case is "flat," that is, a constant function. Thus, in this case, a superior estimate of each $\gamma(h_k)$ is given by the weighted average

$$\overline{\gamma}_{\text{FUSD}} = \frac{\sum_{k=1}^{K_{\mathcal{U}}} N(\mathcal{U}_k) \hat{\gamma}_{\text{FUSD}}(h_k)}{\sum_{k=1}^{K_{\mathcal{U}}} N(\mathcal{U}_k)}.$$

On the other hand, if $Y(\cdot)$ is pure tail-down or a mixture of tail-up and tail-down, then the flow-unconnected portion of its semivariogram may be a function not of total stream distance but of the two stream distances from sites within a site-pair to their common junction, in which case $\hat{\gamma}_{\text{FUSD}}(\cdot)$ may not be fully relevant, that is, what it purports to estimate does not exist. An exception occurs if the tail-down component has an exponential semivariogram; in this case the flow-unconnected portion of its semivariogram *is* a function of total stream distance only (see Table 1), hence $\hat{\gamma}_{\text{FUSD}}(\cdot)$ remains unbiased for it (apart from blurring).

3.1.2 The Flow-Unconnected Distances-to-Common-Junction (FUDJ) Semivariogram

The second component semivariogram of the Torgegram, like the first, is computed using only those site-pairs that are flow-unconnected, but it is not a function of total stream distance. Rather, it is a function of the two stream distances from each site in the pair to their common junction. Let $\{\mathcal{J}_k : k = 1, \ldots, K_{\mathcal{J}}\}$ be the bins of a partition of the stream distances to common junction that occur among the flow-unconnected site-pairs, let $N(\mathcal{J}_k, \mathcal{J}_l)$ be the number of such site-pairs for which one site's distance to common junction lies in $\mathcal{J}_k$ and the other's lies in $\mathcal{J}_l$, and let j_k be a representative distance within $\mathcal{J}_k$. Without loss of generality, assume that $j_k \leq j_l$. Then we define the flow-unconnected distances-to-common-junction empirical semivariogram as

$$\hat{\gamma}_{\text{FUDJ}}(j_k, j_l) = \frac{1}{2N(\mathcal{J}_k, \mathcal{J}_l)} \sum_{s_i \in \mathcal{J}_k,\, t_j \in \mathcal{J}_l} (Y(s_i) - Y(t_j))^2, \quad k \leq l = 1, \ldots, K_{\mathcal{J}}.$$

Regardless of whether $Y(\cdot)$ is pure tail-down, pure tail-up, or a mixture thereof, $\hat{\gamma}_{\text{FUDJ}}(\cdot, \cdot)$ is unbiased (apart from blurring)

for the flow-unconnected portion of its semivariogram. This is its advantage over $\hat{\gamma}_{\text{FUSD}}(\cdot)$, which (as noted previously) is not fully relevant unless $Y(\cdot)$ is pure tail-up or its tail-down component has an exponential semivariogram. However, because $\hat{\gamma}_{\text{FUDJ}}(\cdot,\cdot)$ is a function of two distances rather than one, it must be displayed in three dimensions (unless contour or gray-scale plotting is used). Hence, it is a bit more cumbersome to plot and examine than $\hat{\gamma}_{\text{FUSD}}(\cdot)$. Furthermore, due to a reduction in sample sizes within bins it has greater uncertainty, as each $\hat{\gamma}_{\text{FUDJ}}(j_k, j_l)$ is generally computed from a subset of the site-pairs used to compute the corresponding $\hat{\gamma}_{\text{FUSD}}(h_k)$.

3.1.3 The Flow-Connected Stream-Distance (FCSD) Semivariogram and Its Subsemivariograms

The FCSD semivariogram is based on stream distance only but differs from the FUSD semivariogram by being computed from site-pairs that are flow-connected rather than flow-unconnected. Thus, it is defined as

$$\hat{\gamma}_{\text{FCSD}}(h_k) = \frac{1}{2N(\mathcal{C}_k)} \sum_{(s_i,t_j)\in\mathcal{C}_k} (Y(s_i) - Y(t_j))^2, \quad k = 1, \ldots, K_{\mathcal{C}},$$

where $\mathcal{C}_k = \{(s_i, t_j) : d(s_i, t_j) \in \mathcal{H}_k,\ U_i \cap U_j \neq \emptyset\}$, h_k is a representative distance within $\mathcal{C}_k$, $N(\mathcal{C}_k)$ is the number of distinct site-pairs in $\mathcal{C}_k$, and $K_{\mathcal{C}}$ is the number of stream-distance bins for those site-pairs. If $Y(\cdot)$ is pure tail-down, then $\hat{\gamma}_{\text{FCSD}}(\cdot)$ is unbiased (apart from blurring) for the flow-connected portion of its semivariogram. If, however, $Y(\cdot)$ is pure tail-up or a tail-up/tail-down mixture, $\hat{\gamma}_{\text{FCSD}}(\cdot)$ is not fully relevant because in those cases the flow-connected semivariogram is a function of not merely stream distance, but stream distance and the spatial weights. An empirical semivariogram that accounts for the weights and can therefore estimate the unweighted flow-connected semivariogram of a tail-up $Y(\cdot)$ unbiasedly is described in the next subsection.

Although $\hat{\gamma}_{\text{FCSD}}(\cdot)$ may not be fully relevant unless $Y(\cdot)$ is pure tail-down, it can be decomposed into empirical "subsemivariograms," of which one is fully relevant regardless of the nature of the dependence of $Y(\cdot)$. These subsemivariograms are based on a partition $\{\mathcal{C}_{k0}, \mathcal{C}_{k1}, \ldots, \mathcal{C}_{kq_k}\}$ of each $\mathcal{C}_k$ into sets of flow-connected site-pairs separated within the stream network by 0, 1, …, or q_k junctions, respectively. Thus, site-pairs belonging to $\mathcal{C}_{k0}$ lie within the same stream segment, site-pairs belonging to $\mathcal{C}_{k1}$ are situated such that one of the sites lies on the segment immediately downstream of the other site, and so on. We define the FCSD Type-p subsemivariogram of $Y(\cdot)$, or FCSD-p for short, as

$$\hat{\gamma}_{\text{FCSD},p}(h_k) = \frac{1}{2N(\mathcal{C}_{kp})} \sum_{(s_i,t_j)\in\mathcal{C}_{kp}} (Y(s_i) - Y(t_j))^2, \quad k = 1, \ldots, K_{\mathcal{C}}.$$

FCSD-0 is unbiased for the flow-connected portion of the semivariogram of $Y(\cdot)$, regardless of whether $Y(\cdot)$ is pure tail-down, pure tail-up, or some mixture thereof. (This is not unlike the way that a "pure error" mean square from the analysis of variance (ANOVA) of a regression model is unbiased for the residual variance regardless of whether the regression function is correctly specified.) FCSD-1, FCSD-2, … do not share this nice property. Note that for FCSD-0 to exist, some stream segments must contain multiple observation sites. Also note that all of the subsemivariograms have greater uncertainty than the intact FCSD semivariogram, due to reduced sample sizes within bins.

3.1.4 The Flow-Connected Weight-Adjusted (FCWA) Semivariogram

The FCSD semivariogram described in Section 3.1.3 does not account for the spatial weights, which causes no problems if $Y(\cdot)$ is pure tail-down, but leads to a biased estimate of the unweighted flow-connected semivariogram otherwise. This bias may, in particular, adversely affect the analyst's ability to determine the range of spatial dependence among flow-connected sites from $\hat{\gamma}_{\text{FCSD}}(\cdot)$. To illustrate, consider an example based on the idealized dyadic stream network depicted in Figure 1. This network comprises seven segments of equal length 1.0, with both segments at each junction weighted equally. Suppose that five observations are taken on each segment (for a total sample size of 35) at distances 0.1, 0.3, 0.5, 0.7, and 0.9 units above its downstream terminus, and that $Y(\cdot)$ is pure tail-up with unweighted flow-connected portion given by an exponential model having variance 1.0 and correlation at distance 1.0 equal to $\rho = 0.25$, 0.50, or 0.75. Table 2a displays the value of this model and the expected value of the FCSD semivariogram at selected distances. Comparison of these two values at each distance indicates that the FCSD semivariogram is positively biased at all distances, and that at each fixed distance the bias gets worse as the spatial correlation gets stronger. Note that the effects of

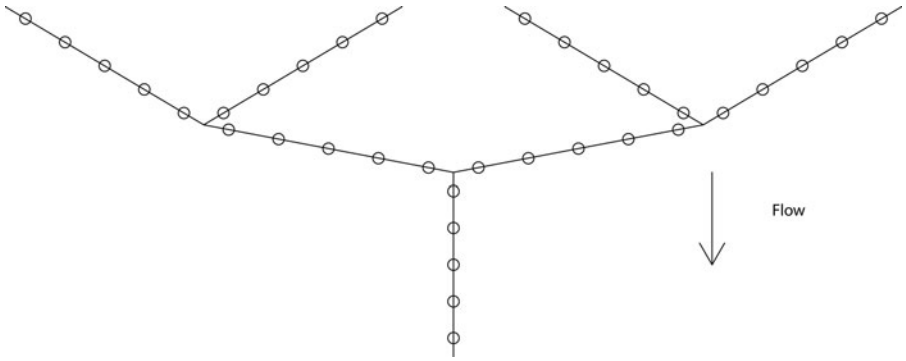

Figure 1. Stream network and sample locations for Example 1.

Table 2. Bias, for the examples described in Section 3.1.4, of (a) the empirical FCSD semivariogram, and (b) the empirical FCWA semivariogram.

(a)		Distance (h)			
ρ	Semivariogram	0.2	0.6	1.0	1.4
0.25	$\gamma_{uw}(h)$	0.242	0.565	0.750	0.856
0.25	$E(\hat{\gamma}_{\text{FCSD}}(h))$	0.281	0.637	0.823	0.908
0.50	$\gamma_{uw}(h)$	0.129	0.340	0.500	0.621
0.50	$E(\hat{\gamma}_{\text{FCSD}}(h))$	0.175	0.449	0.647	0.756
0.75	$\gamma_{uw}(h)$	0.056	0.159	0.250	0.332
0.75	$E(\hat{\gamma}_{\text{FCSD}}(h))$	0.105	0.297	0.470	0.570
(b)		Distance (h)			
ρ	Semivariogram	0.2	0.6	1.0	1.4
0.25	$\gamma_{fc}(h)$	0.242	0.565	0.750	0.856
0.25	$E(\hat{\gamma}_{\text{FCWA}}(h))$	0.195	0.504	0.693	0.838
0.50	$\gamma_{fc}(h)$	0.129	0.340	0.500	0.621
0.50	$E(\hat{\gamma}_{\text{FCWA}}(h))$	0.087	0.267	0.410	0.564
0.75	$\gamma_{fc}(h)$	0.056	0.159	0.250	0.332
0.75	$E(\hat{\gamma}_{\text{FCWA}}(h))$	0.028	0.104	0.174	0.271

this on the characterization of the nugget and sill would be minimal; however, it could cause the effective range to be underestimated somewhat. Incidentally, the case of equal weights considered in this example is a best-case scenario; the bias is slightly larger if the weights are unequal.

If the weights are known, it is possible to modify the empirical semivariogram to yield an unbiased estimator of the unweighted flow-connected semivariogram, as follows. Define

$$\hat{\gamma}_{\text{FCWA}}(h_k) = \overline{\gamma}_{\text{FUSD}} - \frac{1}{2N(\mathcal{C}_k)} \times \sum_{(s_i,t_j)\in\mathcal{C}_k} \frac{2\overline{\gamma}_{\text{FUSD}} - [Y(s_i) - Y(t_j)]^2}{\pi_{ij}}, \quad k = 1, \ldots, K_{\mathcal{C}}.$$

It can be verified that $\hat{\gamma}_{\text{FCWA}}(\cdot)$ estimates unbiasedly (apart from blurring) the unweighted flow-connected portion of the semivariogram of a pure tail-up $Y(\cdot)$. Of course, if $Y(\cdot)$ is not pure tail-up, then $\hat{\gamma}_{\text{FCWA}}(\cdot)$ is biased. Table 2(b) lists the expectations of $\hat{\gamma}_{\text{FCWA}}(\cdot)$ for an example identical to that described in the previous paragraph except that $Y(\cdot)$ is pure tail-down rather than pure tail-up. These indicate that the FCWA semivariogram is negatively biased under a pure tail-down model.

Although the FCWA semivariogram is unbiased under a pure tail-up model, its variability can be unacceptably high. To illustrate, we simulated a stream network with 500 segments, each of length 1, and generated 400 samples completely randomly placed on the network (left side of Figure 2) using the SSN package (Ver Hoef et al. 2014) in R (R Core Team 2015). For the 400 samples, we simulated autocorrelated data from a linear-with-sill tail-up model (Table 1), with a partial sill of 1, a range of 10, and a nugget of 0.01. We created 5000 realizations on the fixed set of locations. Figure 2 (right side) displays boxplots of the values of $\hat{\gamma}_{\text{FCWA}}(h_k)$ compared to $\hat{\gamma}_{\text{FCSD}}(h_k)$ for distances in bins of width 2, up to a maximum distance of 20. Although the results verify that $\hat{\gamma}_{\text{FCWA}}$ is unbiased, they also indicate that it can vary wildly. In fact, the empirical mean squared error of $\hat{\gamma}_{\text{FCWA}}(h_k)$ is much larger (by a factor of more than 100 at some lags) than that of $\hat{\gamma}_{\text{FCSD}}(h_k)$, and the medians for reasonable lag distances ($13 < h < 22$) are less than 0, for this example. The high variance is caused by dividing by small values of π_{ij} when computing $\hat{\gamma}_{\text{FCWA}}(h_k)$. Further research is needed on alternative estimators of the unweighted flow-connected portion of the semivariogram of a pure tail-up model that balance bias and variance better than $\hat{\gamma}_{\text{FCWA}}(\cdot)$ does. Pending the results of this research, at the present time we recommend using $\hat{\gamma}_{\text{FCSD}}(\cdot)$ without modification to characterize flow-connected dependence, despite its bias. Furthermore, in the graphical display of the Torgegram, we use the position that would otherwise be occupied by the FCWA semivariogram to display the FCSD-0 and FCSD-1 subsemivariograms.

3.2 Trend Contamination

All claims we have made to this point regarding the bias of various Torgegram components are based on a model in which the mean of $Y(\cdot)$ is constant. Suppose now that the mean is actually

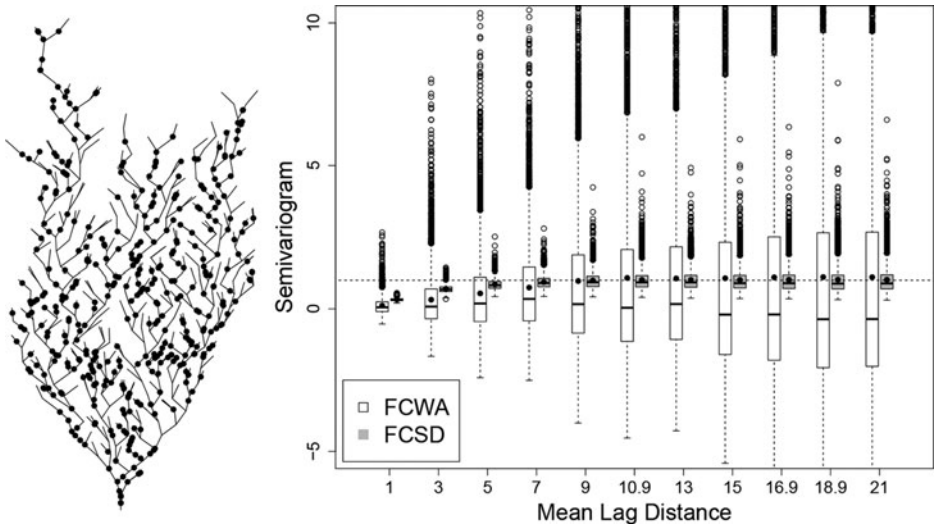

Figure 2. Boxplots of FCWA and FCSD for simulated data. The simulated stream network is shown on the left with black circles indicating the random sample locations. Boxplots on the right use a solid horizontal line to show the median, and a solid circle for the mean.

a linear function of upstream distance, but that this is unknown to the analyst. That is, suppose the analyst acts as though $Y(\cdot)$ follows the model given by (2) and (5), that is,

$$Y(s_i) = \mu + \epsilon_{tu}(s_i) + \epsilon_{td}(s_i) + \nu(s_i),$$

when actually

$$Y(s_i) = \mu + \beta s + \epsilon_{tu}(s_i) + \epsilon_{td}(s_i) + \nu(s_i).$$

Then the expected value of a generic term, $(Y(s_i) - Y(t_j))^2$, in any of the Torgegram's component empirical semivariograms is given by

$$\begin{aligned} 2\gamma(s_i, t_j) &= E\{[\mu + \beta s + \epsilon_{tu}(s_i) + \epsilon_{td}(s_i) + \nu(s_i) - \mu \\ &\quad -\beta t - \epsilon_{tu}(t_j) - \epsilon_{td}(t_j) - \nu(t_j)]^2\} \\ &= \beta^2(s-t)^2 + E[(\epsilon_{tu}(s_i) - \epsilon_{tu}(t_j))^2] \\ &\quad +E[(\epsilon_{td}(s_i) - \epsilon_{td}(t_j))^2] \\ &\quad +E[(\nu(s_i) - \nu(t_j))^2]. \end{aligned}$$

For the sake of simplicity, suppose that the semivariogram of the tail-down component is exponential, so that both its flow-connected and flow-unconnected portions are functions of total stream distance only. Now recall that if sites s_i and t_j are flow-connected, then $d(s_i, t_j) = |s - t|$. However, if s_i and t_j are flow-unconnected, then $d(s_i, t_j) = s + t - 2q_{ij} > |s - t|$ and the difference between the two can be large, particularly if the network is strongly dendritic (in which case $|s - t|$ can be as small as 0, even when $s + t - 2q_{ij}$ is large). Writing $\sigma^2 = \sigma_{tu}^2 + \sigma_{td}^2 + \sigma_{nu}^2$, we may therefore rewrite $2\gamma(s_i, t_j)$ as follows:

$$2\gamma(s_i, t_j) = \begin{cases} 0 & \text{if } s_i = t_j, \\ \beta^2[d(s_i, t_j)]^2 + 2\sigma^2 - 2C_{tu}(d(s_i, t_j)|\{\pi_{ij}\}) & \\ \quad -2C_{td}(d(s_i, t_j)) & \text{if } s_i \neq t_j \text{ are flow-connected,} \\ \alpha_{ij}\beta^2[d(s_i, t_j)]^2 + 2\sigma^2 & \\ \quad -2C_{td}(d(s_i, t_j)) & \text{if } s_i, t_j \text{ are flow-unconnected,} \end{cases}$$

where $\alpha_{ij} = (s-t)^2/[d(s_i, t_j)]^2 \in (0, 1)$ for all flow-unconnected segments i and j. Thus, in this scenario, smooth curves drawn through the FUSD and FCSD components of the Torgegram will increase without bound. Moreover, FUSD will tend to have a larger nugget, but less curvature, than FCSD, so that at some point the two curves will cross (see Figure 3). This manner of unboundedness and crossing of these two components of the Torgegram may therefore be taken as evidence of an unmodeled trend in upstream distance, just as an empirical Euclidean semivariogram that increases without bound is often taken as evidence of an unmodeled planar trend; see, for example, Starks and Fang (1982).

What if the trend is related instead to covariates that do not change in an upstream direction? For example, what if there are differences in water chemistry due to gradual changes in bedrock formations that lie orthogonal to the general direction of flow? In this scenario, a similar analysis indicates that $2\gamma(s_i, t_j)$ is given by an expression almost identical to that in the first scenario; the only difference is that the term $\beta^2(s-t)^2$ is replaced by $\beta^2[x(s_i) - x(t_j)]^2$, where $x(s_i)$ and $x(t_j)$ are the coordinates of sites s_i and t_j, within a Euclidean coordinate system, in the direction orthogonal to flow. Thus, FUSD will again have larger nugget, and both of FUSD and FCSD will increase without bound, as in the previous scenario. However, the degree of curvature in this case will be no less for FUSD than for FCSD, so there will be no crossing of curves as there is when the trend is aligned with flow.

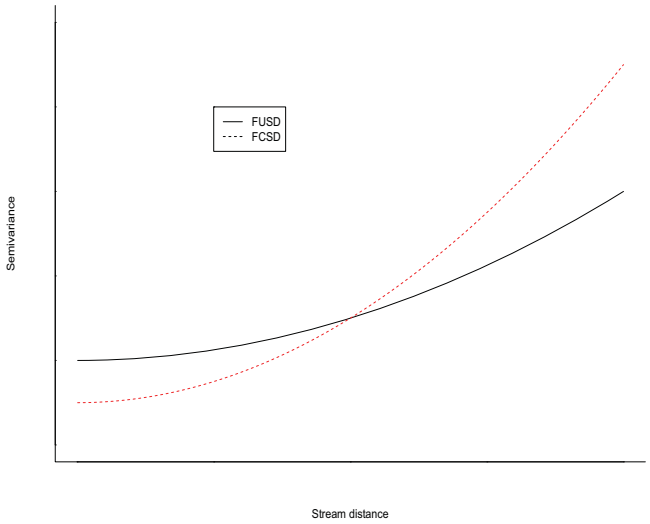

Figure 3. Effects of aligned-with-flow trend contamination on the FUSD and FCSD components of the Torgegram.

3.3 A Strategy for Fluvial Variography

Each of the four component semivariograms of the Torgegram is relevant for unbiasedly estimating (apart from blurring) either the flow-connected or flow-unconnected portion of the semivariogram of some, but not all, cases of the mixed tail-up/tail-down family of models. In particular, $\hat{\gamma}_{\text{FUSD}}(\cdot)$ and $\hat{\gamma}_{\text{FCWA}}$ are unbiased for the corresponding portions of the semivariogram when $Y(\cdot)$ is pure tail-up, and $\hat{\gamma}_{\text{FUDJ}}(\cdot, \cdot)$ and $\hat{\gamma}_{\text{FCSD}}(\cdot)$ are unbiased for the corresponding portions of the semivariogram when $Y(\cdot)$ is pure tail-down. In practice, of course, the make-up of the covariance structure of $Y(\cdot)$ is unknown to the analyst, and a strategy is needed for using the Torgegram to sort it all out. We propose that this be accomplished along the following lines.

1. Examine the FUSD semivariogram. If it appears to increase without bound, add a trend term (in upstream distance if FUSD crosses FCSD, or in the coordinate aligned orthogonally to flow otherwise) to the model and recompute this semivariogram from the fitted residuals. If it appears to be relatively flat, adopt a pure tail-up model and determine its attributes using the FUSD and FCSD semivariograms. Rough estimates of the sills may be determined from both semivariograms, while rough estimates of a nugget and range (or effective range) for $C_{uu}(\cdot)$ may be determined from the latter (keeping in mind that the range as determined from $\hat{\gamma}_{\text{FCSD}}$ may be underestimated), essentially completing the informal stage of the variographic exercise. If the FUSD semivariogram appears to be bounded but not flat, conclude that

a pure tail-up model is not adequate and proceed to the next step.

2. Examine the FCSD semivariogram and, if possible, its subsemivariograms; in practice, only some of the subsemivariograms might be reliable enough to be worth examining. If the subsemivariograms appear to be relatively similar, then adopt a pure tail-down model and use the FCSD semivariogram unambiguously to roughly determine a sill, range, and nugget for the flow-connected portion of the semivariogram. Otherwise, conclude that the model is a mixture of tail-up and tail-down components and proceed (after the next step) with a formal model fitting and selection exercise to determine an appropriate mixture and estimate parameters associated with each component.
3. Examine the FUDJ semivariogram, using the manner in which it varies across bins (j_k, j_l) corresponding to the same total stream distance $j_k + j_l$ to guide model choice for the tail-down component in the mixed model. For example, if it appears to be similar across all such bins, then adopt an exponential model for the tail-down component.

Effective implementation of this strategy requires that the component semivariograms of the Torgegram are estimated reliably. Here, as in Euclidean geostatistics, the reliability of an estimated semivariance corresponding to a certain lag distance bin depends on (1) the lag distance itself, (2) the number of site-pairs in the bin, and (3) the strength of the spatial dependence in the process $Y(\cdot)$. (The reliability is inversely related to the first and third of these, and directly related to the second.) Although the analyst generally has no control over the strength of spatial dependence, (s)he does have some control over the other two factors. Within Euclidean geostatistics, a long-standing rule of thumb is to estimate the semivariogram at only those lag distances whose bins contain at least 25 site-pairs and that are less than half the maximum distance between sites; see, for example, Journel and Huijbregts (1978). We recommend following the same rule for the minimum number of site-pairs for all component semivariograms of the Torgegram. For the subsemivariograms of FCSD, however, this will generally be much more difficult to attain unless some stream segments are sampled intensively, which is not common in practice (but perhaps it should be!). Consequently, we recommend relaxing this standard to perhaps 5–10 site-pairs (within a concomitant weakening of the force of conclusions) for FCSD-0 and other subsemivariograms. As for the maximum lag distance at which to estimate the semivariograms, our recommendation varies across the component semivariograms of the Torgegram. For FCSD and its subsemivariograms, we see no reason not to adapt the Euclidean recommendation straightforwardly, that is, to one-half the maximum stream distance between flow-connected sites, say $\breve{d}_{\mathrm{FC}}/2$. For FUSD and FUDJ, we would not argue with a similar recommendation of one-half the maximum total stream distance between flow-unconnected sites, which will tend to be somewhat larger than $\breve{d}_{\mathrm{FC}}/2$. However, in the example presented later, for the sake of consistency and an easier graphical comparison, we will use a maximum lag total stream distance of $\breve{d}_{\mathrm{FC}}/2$ for these two components also.

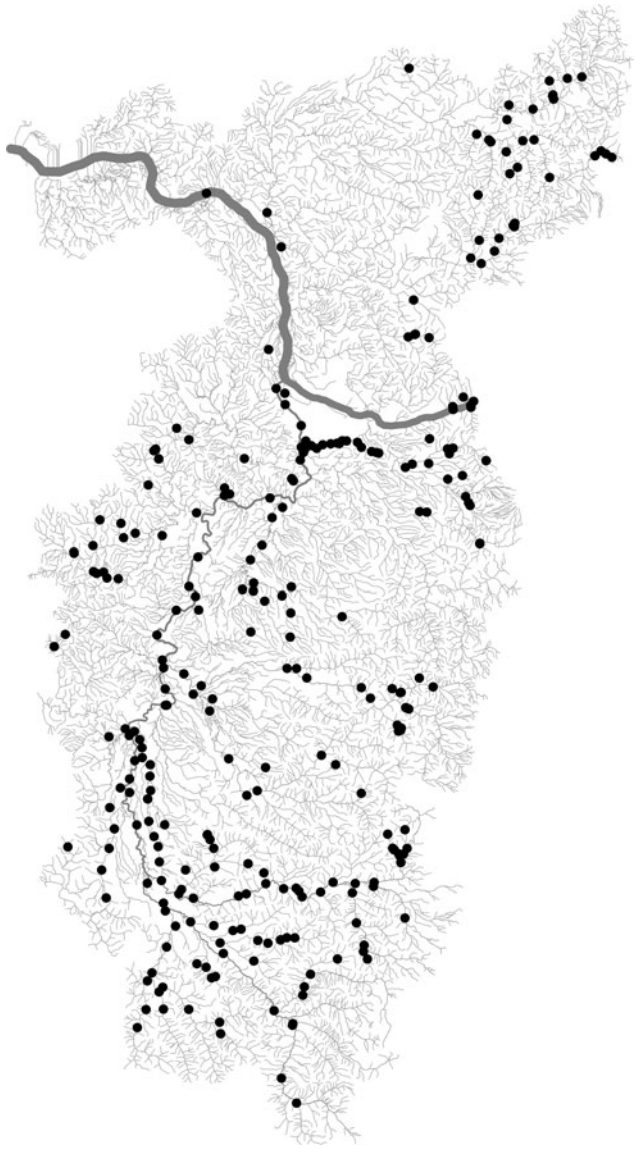

Figure 4. Data locations for the Lewis and Willamette watersheds stream temperature data. These watersheds lie within the Columbia River basin in the northwest United States; the thickest line indicates the Columbia River. The Lewis river is to the north (up) and the Willamette river is to the south (down). Data locations for 286 temperature loggers from 2002 are shown by solid circles.

4. Example: Stream Temperature in the Lewis and Willamette Watersheds

To illustrate the use of the Torgegram in a real example, stream temperature data were downloaded from the NorWeST website, *http://www.fs.fed.us/rm/boise/AWAE/projects/NorWeST.html*, which hosts >150 million hourly stream temperature recordings from >100 natural resource agencies in the western U.S. These data were collected using digital sensors that recorded >10 water temperature measurements per day and have passed through a consistent set of quality-assurance procedures as described in metadata descriptions at the project website. We used data taken in 2002 from 286 locations on two watersheds, the Lewis and Willamette, connected to the Columbia River, USA, which forms the border between the states of Washington and Oregon (Figure 4). Raw temperature measurements (in degrees Celsius) were averaged over the

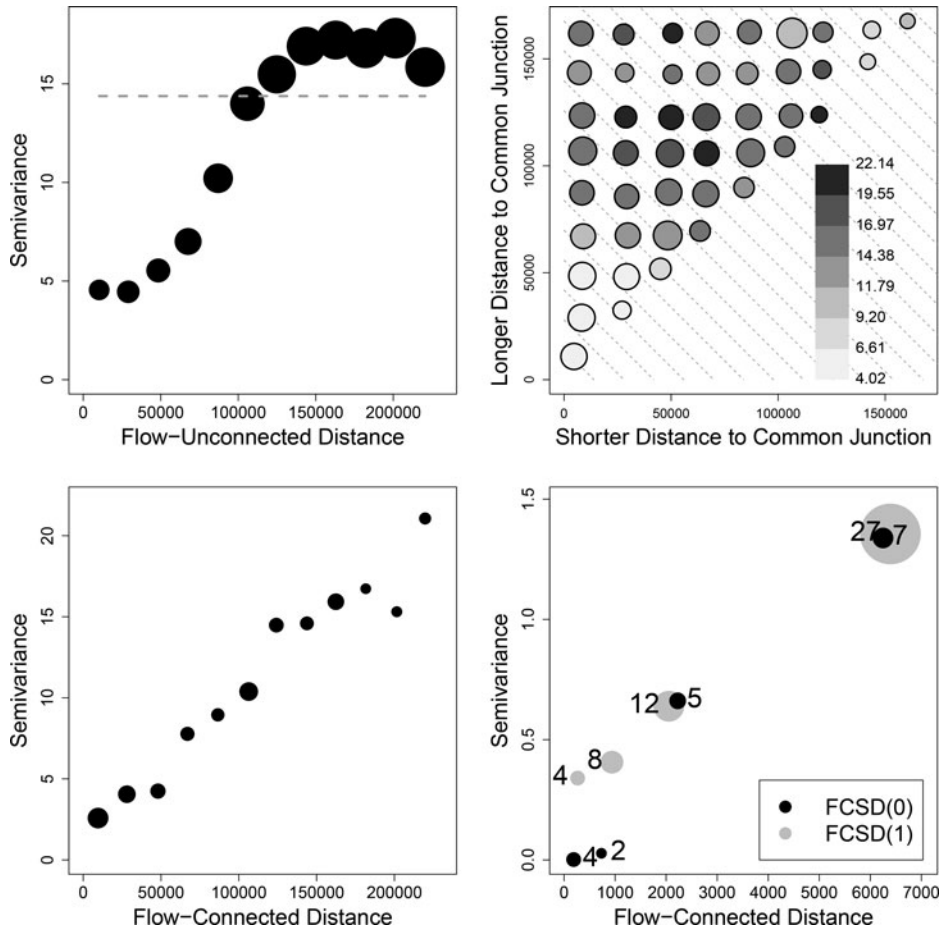

Figure 5. Torgegrams for the Lewis and Willamette watersheds stream temperature data. Upper left panel is FUSD where the dashed horizontal line is the weighted mean FUSD value; upper right is FUDJ where diagonal dashed lines show equal total stream distance and the legend strip partitions the range of observed semivariances; lower left is FCSD; and lower right is FCSD-0 compared to FCSD-1. In all panels, diameters of the circles are proportional to the number of pairs of points in each bin, which range from 293 to 1953 for FUSD, 30 to 524 for FUDJ, and 225 to 377 for FCSD. In the lower right panel, actual number of pairs of points are printed, with Type-0 given to the right of the circle, and Type-1 to the left of the circle.

period 1–31 August, which is the warmest part of the annual cycle and provides a good metric of overall thermal suitability for fish (Isaak et al. 2010). The 1:100,000-scale National Hydrography Dataset-Plus (NHD-Plus) geospatial layer (*http://www.horizon-systems.com/NHDPlus/index.php*) has been reconditioned with STARS software (Peterson and Ver Hoef 2014) to create the National Stream Internet (NSI, *http://www.fs.fed.us/rm/boise/AWAE/projects/NationalStreamInternet.html*). The temperature data were snapped to NSI streams, and the π_{ij} in (3) used watershed proportions (Peterson and Ver Hoef 2014).

For the temperature data, we created 12 total stream distance classes for the Torgegram with bins of equal size up to a maximum distance of 230,000 m, which was approximately one-half the maximum distance among flow-connected sites. FUSD (Figure 5, upper left) shows clear indication of autocorrelation, with a sill appearing at approximately 17°C^2 and a range near 150,000 m. FCSD (Figure 5, lower left) increases linearly without bound and crosses both FUSD and its apparent sill. FCSD-0 (Figure 5, lower right) shows nearly zero nugget effect as semivariances within stream segments are nearly zero at short distances, but there does appear to be a small jump in semivariances when crossing junctions (FCSD-1) for those same distances. FUDJ (Figure 5, upper right) also shows semivariances generally increasing with total stream distance. Interestingly, the semivariances also appear to increase when moving up and to the left along the diagonal lines, especially for smaller distances. This indicates that semivariances are higher for equal total stream distances when there is more asymmetry in the distances to the common junction. This is also a feature of many tail-down model constructions (Garreta, Monestiez, and Ver Hoef 2010), although, until now, no one has checked to see if data actually adhere to the model.

Following our fluvial variography strategy outlined earlier, it is clear that the FCSD curve is unbounded and crosses the FUSD curve (Figure 5), indicating trend contamination aligned with flow. Consequently, we fit a model (by ordinary least squares) that included both distance upstream and elevation as regressors. From the residuals of this fit, we recomputed the various components of the Torgegram (Figure 6). FUSD (Figure 6, upper left) still indicates autocorrelation, but the sill and range are smaller (approximately 7°C^2 and 100,000 m, respectively) than they were for the raw data (compare to Figure 5). FCSD (Figure 6, lower left) is no longer unbounded but increases asymptotically toward what should be the same sill as in FUSD. FCSD-0 (Figure 6, lower right) again shows nearly zero nugget effect as semivariances within stream segments are nearly zero at short distances, but there does again appear to be a small jump

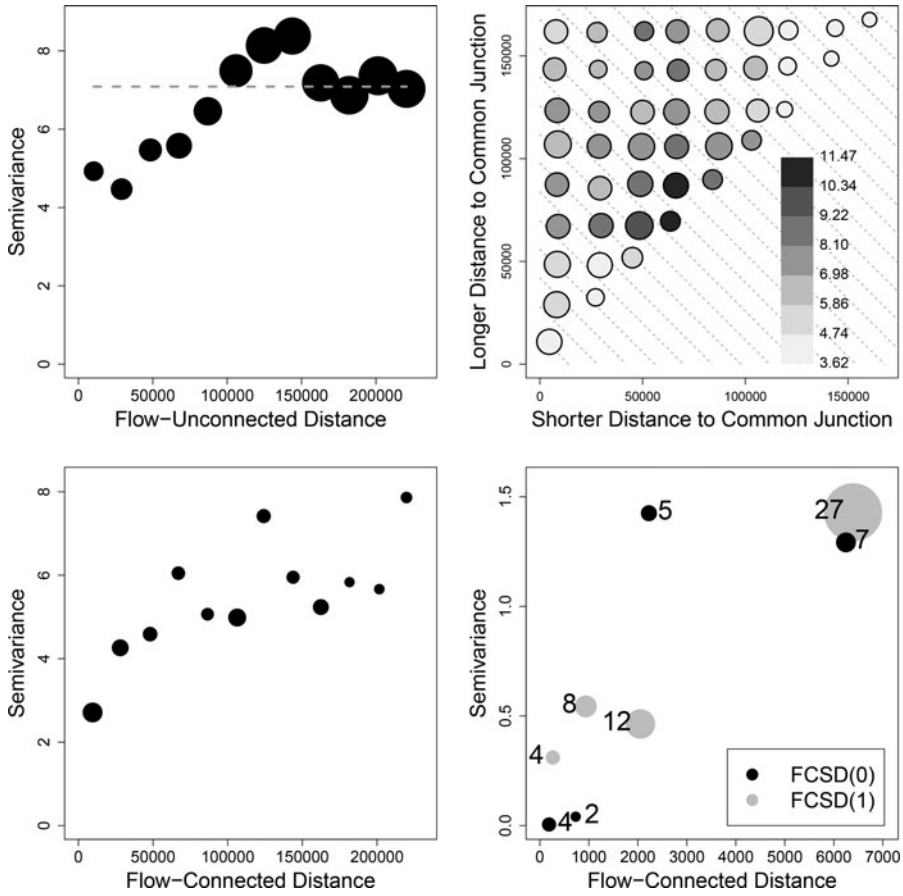

Figure 6. Torgegrams for residuals, after removing effects for distance upstream and elevation, of the Lewis and Willamette watersheds stream temperature data. The description is exactly as for Figure 5.

when crossing junctions for those same distances. However, the subsemivariograms' sample sizes are so small, especially for FSCD-0, that a jump of this magnitude might be attributable to chance. FUDJ (Figure 6, upper right) again shows semivariances generally increasing with total stream distance. However, they no longer appear to increase when moving up and to the left along the diagonal lines; in fact, for medium distance classes they appear to do the opposite.

Informed by our Torgegram-based exploratory fluvial variography, we fitted two models to the data. For the first model, we used fixed effects for distance upstream and elevation and a pure spherical tail-up model for the second-order dependence. Although FUSD does not appear to be very flat, indicating some autocorrelation (Figure 6, upper left) among flow-unconnected sites, this model provides a null model to compare to the second model. Histograms of residuals appeared to be approximately normal, so we fitted the model by restricted maximum likelihood (REML, Patterson and Thompson 1971) using the SSN package. As predicted by the Torgegram (FCSD-0, Figure 6, lower right) the estimated nugget effect was small (0.797), with an overall sill of 6.885 and a range of 228,557 m. The Akaike Information Criterion value (AIC, Akaike 1973) was 1237.2. We fitted a second model, again using REML, which included the same fixed effects but characterized the second-order dependence by a mixed model of the form specified by (5) and (6), with a spherical tail-up component and a linear-with-sill tail-down component. We chose these models because it is easy to interpret their range parameters, which estimate the distance at which the autocorrelation vanishes; we did not find better fits using models in which the sill is approached asymptotically, such as the exponential and Mariah models. The estimated nugget effect was 0.732, with an overall sill of 8.075. The partial sill for the tail-up spherical model was 3.077 with a range of 599,772 m and the partial sill for the tail-down linear-with-sill model was 4.266 with a range of 99,970 m. The AIC value was 1198.4, indicating a substantially better fit than the first model. The second fitted model seems reasonable given the Torgegram in Figure 6.

5. Discussion

We have developed a graphical diagnostic, called the *Torgegram*, for characterizing spatial dependence among observations of a variable on a stream network. The Torgegram consists of four component empirical semivariograms, each one corresponding to a particular combination of flow-connectedness and model type (tail-up/tail-down). We have shown how an overall strategy for fluvial variography can be based on careful study of the Torgegram, and we carried this out for a stream temperature dataset from two watersheds within the Columbia River basin. A Torgegram consisting of FUSD, FUDJ, and FCSD and its two lowest-level subsemivariograms (FCSD-0 and FCSD-1) has been incorporated, and will be released, in the next version of the R package SSN.

Networks other than stream networks exist, of course. For example, there are neural networks in many animals; vascular networks in many animals and plants; street, highway, and other

transportation networks; municipal water and sewer networks; and communication and social networks. To the extent that these other networks are dendritic and have unidirectional, cumulative flow (e.g., a network of sewer pipes), the Torgegram may be an appropriate tool for describing spatial dependence on them. However, many of these networks are not dendritic (e.g., street networks), and on some of them flow occurs in multiple directions or from a single source to the extremities rather than vice versa (e.g., from the heart to the capillary bed). Further research is needed to develop appropriate graphical tools for characterizing dependence of a spatially continuous process on those types of networks.

We fitted our models using REML, which is standard nowadays. Historically, however, semivariogram models were most often fitted directly to empirical semivariograms using (weighted) least squares (Cressie 1985). REML requires inverting a covariance matrix that has dimensions equal to the sample size, which is a computational limitation. Fitting Torgegrams directly could allow model fits to massive datasets as no matrix inverses are required. We do not fully develop the topic here, however, because more research is needed on appropriate weighting among FUSD, FUDJ, and FCSD values.

Although the Torgegram is focused on spatial dependence within the unique topology of a stream network, the Euclidean semivariogram may, on occasion, still be a useful tool for fluvial variography. For example, suppose that the spatial correlation among values of the stream variable was caused by an unmeasured covariate related to underlying bedrock characteristics. In such a case, a Euclidean distance-based semivariogram may be more informative than the Torgegram for characterizing the variable's spatial dependence. In any case, a comprehensive characterization of spatial dependence in a stream network may be facilitated by using both of them.

Formal hypothesis testing procedures to accompany the Torgegram are needed and are currently under development. For example, we have adapted the Diblasi–Bowman test for spatial independence in Euclidean geostatistics (Diblasi and Bowman 2001) to test for pure tail-up dependence based on a measure of "flatness" of the FUSD semivariogram; details of this test will be reported elsewhere. We are also developing a test for the hypothesis of pure tail-down dependence using a statistic that measures the discrepancy between the FCSD-0 subsemivariogram and the remaining FCSD subsemivariograms. More specifically, we are considering the test statistic

$$T = (\hat{\boldsymbol{\gamma}}_{\text{FCSD},0} - \hat{\boldsymbol{\gamma}}_{\text{FCSD},>0})' \hat{G}^{-1} (\hat{\boldsymbol{\gamma}}_{\text{FCSD},0} - \hat{\boldsymbol{\gamma}}_{\text{FCSD},>0}),$$

where $\hat{\boldsymbol{\gamma}}_{\text{FCSD},0}$ is the vector of FCSD-0 semivariances, $\hat{\boldsymbol{\gamma}}_{\text{FCSD},>0}$ is the vector of semivariances (at the same distances as those in $\hat{\boldsymbol{\gamma}}_{\text{FCSD},0}$) obtained by pooling all FCSD subsemivariograms except Type 0, G is the asymptotic covariance matrix of $\hat{\boldsymbol{\gamma}}_{\text{FCSD},0} - \hat{\boldsymbol{\gamma}}_{\text{FCSD},>0}$, and $\hat{G}$ is an estimate of G obtained by replacing its elements with the corresponding components of the Torgegram. (In practice, FCSD-1 will often be the only subsemivariogram whose semivariances correspond to distances short enough to match those in $\hat{\boldsymbol{\gamma}}_{\text{FCSD},0}$). Under appropriate conditions, the asymptotic distribution of T under the null hypothesis of pure tail-down dependence is chi-square with degrees of freedom equal to the dimension of $\hat{\boldsymbol{\gamma}}_{\text{FCSD},0}$. Work is underway to determine G and the appropriate asymptotic conditions. Other hypotheses of interest for which Torgegram-based tests may be constructed include exponentiality of the tail-down component (using a statistic that measures the discrepancies in FUDJ semivariances corresponding to the same total stream distance), and variance stationarity across the stream network.

Future work will also include extensions of the Torgegram for use with multivariate and spatio-temporal data on stream networks. An extension to multivariate data would consist of not only Torgegrams to describe the spatial dependence of each variable, but also *cross-Torgegrams* comprising flow-connected and flow-unconnected cross-semivariograms to describe the spatial dependence between each pair of variables.

Acknowledgments

The project received financial support from the Center for Global and Regional Environmental Research at the University of Iowa, and from NOAA's National Marine Fisheries Service, Alaska Fisheries Science Center. The findings and conclusions in this article are those of the authors and do not necessarily represent the views of the National Marine Fisheries Service.

Software

Functions computing FUSD, FUDJ, FCSD, FCSD-0, and FCSD-1 have been incorporated into the SSN R package, available on CRAN. An R package containing additional functions, scripts, and data supporting the simulations, analyses, and figures in this article can be found at *https://github.com/jayverhoef/fluvgrm*.

ORCID

Dale L. Zimmerman http://orcid.org/0000-0003-1212-4089

References

Akaike, H. (1973), "Information Theory and an Extension of the Maximum Likelihood Principle," in *Second International Symposium on Information Theory*, eds. B. N. Petrov, and F. Caski, Budapest: Akademiai Kiado, pp. 267–281. [262]

Bunn, S. E., Abal, E. G., Smith, M. J., Choy, S. C., Fellows, C. S., Harch, B. D., Kennard, M. J., and Sheldon, F. (2010), "Integration of Science and Monitoring of River Ecosystem Health to Guide Investments in Catchment Protection and Rehabilitation," *Freshwater Biology*, 55, 223–240. [253]

Chandler, G. L., Wollrab, S. P., Horan, D. L., Nagel, D. E., Parkes, S. L., Isaak, D. J., Horan, D. L., Wenger, S. J., Peterson, E. E., Ver Hoef, J. M., Hostetler, S. W., Luce, C. H., Dunham, J. B., Kershner, J. L., and Roper, B. B. (2016), "NorWeST Stream Temperature Data Summaries for the Western U.S.," Fort Collins, CO: Forest Service Research Data Archive, *https://doi.org/10.2737/RDS-2016-0032*. [253]

Cressie, N. (1985), "Fitting Variogram Models by Weighted Least Squares," *Journal of the International Association for Mathematical Geology*, 17, 563–586. [263]

Cressie, N., Frey, J., Harch, B., and Smith, M. (2006), "Spatial Prediction on a River Network," *Journal of Agricultural, Biological, and Environmental Statistics*, 11, 127–150. [254]

Diblasi, A., and Bowman, A. W. (2001), "On the Use of the Variogram in Checking for Independence in Spatial Data," *Biometrics*, 57, 211–218. [263]

Ganio, L. M., Torgersen, C. E., and Gresswell, R. E. (2005), "A Geostatistical Approach for Describing Spatial Pattern in Stream Networks," *Frontiers in Ecology and the Environment*, 3, 138–144. [254]

Garreta, V., Monestiez, P., and Ver Hoef, J. M. (2010), "Spatial Modelling and Prediction on River Networks: Up Model, Down Model or Both?," *Environmetrics*, 21, 439–456. [261]

Guan, Y., Sherman, M., and Calvin, J. A. (2004), "A Nonparametric Test for Isotropy Using Subsampling," *Journal of the American Statistical Association*, 99, 810–821. [253]

Isaak, D. J., Luce, C. H., Rieman, B. E., Nagel, D. E., Peterson, E. E., Horan, D. L., Parkes, S., and Chandler, G. L. (2010), "Effects of Climate Change and Wildfire on Stream Temperatures and Salmonid Thermal Habitat in a Mountain River Network," *Ecological Applications*, 20, 1350–1371. [261]

Journel, A. G., and Huijbregts, C. J. (1978), *Mining Geostatistics*, London: Academic Press. [260]

Jun, M., and Genton, M. G. (2012), "A Test for Stationarity of Spatio-Temporal Random Fields on Planar and Spherical Domains," *Statistica Sinica*, 22, 1737–1764. [253]

Legleiter, C. J., Lawrence, R. L., Fonstad, M. A., Marcus, W. A., and Aspinall, R. (2003), "Fluvial Response a Decade after Wildfire in the Northern Yellowston Ecosystem: A Spatially Explicit Analysis," *Geomorphology*, 54, 119–136. [254]

McKay, L., Bonedelid, T., Dewald, T., Rea, Z., Johnston, C., and Moore, R. (2012), "National Hydrography Dataset, Version 2 (NHDPlus, V.2): User Guide," EPA Contract #CM130105CT0027. Available at *http://www.horizon-systems.com/nhdplus/* [253]

Money, E., Carter, G. P., and Serre, M. L. (2009), "Modern Space/Time Geostatistics using River Distances: Data Integration of Turbidity and E. coli Measurements to Assess Fecal Contamination along the Raritan River in New Jersey," *Environmental Science & Technology*, 43, 3736–3742. [254]

Okabe, A., and Sugihara, K. (2012), *Spatial Analysis Along Networks: Statistical and Computational Methods*, New York: Wiley. [254]

Patterson, H. D., and Thompson, R. (1971), "Recovery of Interblock Information when Block Sizes are Unequal," *Biometrika*, 58, 545–554. [262]

Peterson, E. E., and Urquhart, N. S. (2006), "Predicting Water Quality Impaired Stream Segments Using Landscape-Scale Data and a Regional Geostatistical Model: A Case Study in Maryland," *Environmental Monitoring and Assessment*, 121, 613–636. [254]

Peterson, E. E., and Ver Hoef, J. M. (2014), "STARS: An ArcGIS Toolset Used to Calculate the Spatial Information Needed to Fit Spatial Statistical Models to Stream Network Data," *Journal of Statistical Software*, 56, 1–17. [261]

R Core Team (2015), *R: A Language and Environment for Statistical Computing*, Vienna: R Foundation for Statistical Computing. [258]

Starks, T., and Fang, J. (1982), "The Effect of Drift on the Experimental Semi-Variogram," *Journal of the International Association of Mathematical Geology*, 14, 309–320. [259]

Torgersen, C. E., Gresswell, R. E., and Bateman, D. S. (2004), "Pattern Detection in Stream Networks: Quantifying Spatial Variability in Fish Distribution," in *Proceedings of the Second Annual International Symposium on GIS Spatial Analyses in Fishery and Aquatic Sciences*, eds. T. Nishida, P. J. Kailola, and C. E. Hollingworth, Saitama, Japan: Fishery GIS Research Group, pp. 405–420. [254]

Ver Hoef, J. M., and Peterson, E. E. (2010), "A Moving Average Approach for Spatial Statistical Models of Stream Networks," *Journal of the American Statistical Association*, 105, 6–18. [254,255]

Ver Hoef, J. M., Peterson, E. E., Clifford, D., and Shah, R. (2014), "SSN: An R Package for Spatial Statistical Modeling on Stream Networks," *Journal of Statistical Software*, 56, 1–45. [258]

Ver Hoef, J. M., Peterson, E. E., and Theobald, D. (2006), "Spatial Statistical Models that Use Flow and Stream Distance," *Environmental and Ecological Statistics*, 13, 449–464. [254]

Wang, L., Infante, D., Esselman, P., Cooper, A., Wu, D., Taylor, W., Beard, D., Whelan, G., and Ostroff, A. (2011), "A Hierarchical Spatial Framework and Database for the National River Fish Habitat Condition Assessment," *Fisheries*, 36, 436–449. [253]

Yaglom, A. M. (1987), *Correlation Theory of Stationary and Related Random Functions* (Vol. I), New York: Springer-Verlag. [254]

Yuan, L. L. (2004), "Using Spatial Interpolation to Estimate Stressor Levels in Unsampled Streams," *Environmental Monitoring and Assessment*, 94, 23–38. [254]